Experimental Investigation of a Novel Direct Mechanical Drive Wave Energy Converter

Vishnu Vijayasankar[1], Gundi Amarnath[2], S. A. Sannasiraj[3], Abdus Samad[4]

Department of Ocean Engineering, Indian Institute of Technology Madras, Chennai 600036, India

[1]vishnuvijayasankar@gmail.com
[2]amarnath.gvm@gmail.com
[3]sasraj@iitm.ac.in
[4]samad@iitm.ac.in

Abstract— **In the present work, a unique design using a direct mechanical drive based power takeoff system is proposed, designed, fabricated and tested for a point absorber. The power take-off mechanism in the design consists of rack and pinion arrangement, which converts the bidirectional reciprocating motion to unidirectional rotation. This mechanism is fixed on top of an oscillating buoy. The model is tested in a 4m wave flume to measure various parameters like Response Amplitude Operator of the buoy, capture width, electric power output and absorption efficiency for different wave height and periods. The model is also tested for friction outside the flume. The experiments revealed some promising results that can be taken forward for further investigations.**

Keywords— **wave energy, point absorber, rack and pinion, power take-off mechanism.**

I. INTRODUCTION

The types of wave energy converters (WECs) are categorized based on their principle of operation, shape or the location. Articles like Cruz [1], Falcao [2] and Clement *et al.* [3] will provide an insight into various existing energy converters. Point absorbers are wave energy converters with its horizontal length much smaller than the wavelength and convert the heave motion of the buoy imparted from the waves into linear or rotational motion, which in turn is used to run an electric generator with the help of a power takeoff mechanism (PTO). These type of WECs are advantageous since they can extract energy from a wavefront of length much more than their geometric width [4].

PTO mechanism, which is the most fundamental component of a WEC, converts the absorbed wave energy into electricity. Wave energy is absorbed by using systems like Oscillating Water Columns (OWC) or buoys. The PTO system not only determines the efficient conversion of absorbed power but also affects the mass, the size and the structural dynamics of the whole system [5].

The flow paths of different PTOs are shown in Fig. 1.

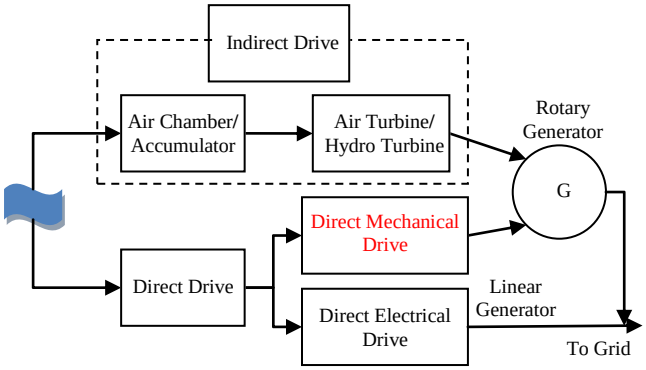

Fig. 1 Flow paths for different PTO mechanisms

Out of all PTO mechanisms, the most widely used one is the air turbine coupled to an oscillating water column, which is an indirect drive mechanism. Even though it has high reliability due to simplicity in working, the efficiency is very low [2][6]. Pelamis [7] uses another indirect drive method using accumulators and rotary generators. However, compared to OWCs, this system lacks reliability and is prone to leakage problems.

Since, in direct drive systems, only up to three energy conversions are required, these systems have higher efficiency. A direct electrical drive system usually consists of a linear generator that directly converts the reciprocating motion into electricity. This PTO is successfully used in different projects like Lysekil Project [8]. However, in the case of direct electrical system, the highly precise design is required since fine air gaps are to be maintained between the stator and translator. Thus, direct mechanical system gets an edge over other forms of PTO in terms of efficiency and simplicity. For the same reason, direct mechanical drive System is chosen to be the PTO mechanism for the present work.

Some notable work is been done in the field of direct mechanical drive PTO mechanisms. In 2011, *H. Karayaka et al* [9] proposed a system using components of an IC engine to drive a rotary generator. But, the system was very complex and it was idle in the occasion where the wave breaks before reaching the system. In 2013, a project named Lifesaver was proposed by *J. Sjolte et al* [10] that uses a winch and rope system coupled to a rotary generator as the PTO system. The main disadvantage of this system was that the generator can

only produce power during upwards motion. In 2015, *J. Ai et al* [11] proposed a system that uses a mechanical motion rectifier mechanism as the PTO. Compared to other direct mechanical drive systems, this system proved to be simpler and efficient. But, here the weight of the PTO and generator is supported by buoy, reducing system efficiency. In the present work, the same idea is conceived for PTO, but the design is altered so that weight of generator is supported separately by the spar. Thus the buoy will experience lesser damping and enhanced heave response.

II. NOMENCLATURE

Abbreviations

WEC	Wave Energy Converter
PTO	Power Take-off
OWC	Oscillating Water Columns
RAO	Response Amplitude Operator
DAQ	Data Acquisition System
MMR	Mechanical Motion Rectifier
SS	Stainless Steel

Symbols

b_d	damping coefficient [kg rad/s]
F_A	amplitude of harmonic force [m]
ω	angular frequency [rad/s]
k	stiffness [N/m]
m	mass [kg]
ω_n	natural frequency [rad/s]
b_c	critical damping coefficient [kg rad/s]
ζ_d	damping ratio
F_{ex}	excitation force [N]
F_{rad}	radiation force [N]
$F_{hyddamp}$	hydrodynamic damping force [N]
F_{exdamp}	external damping force [N]
F_{res}	restoring force [N]
ρ	density of water [kg/m^3]
ζ	heave amplitude [m]
η	wave amplitude [m]
λ	capture width [m]
P_{abs}	absorbed power [W]
P_{wave}	wave power [W]
F_{fric}	frictional force [N]
m_t	accelerated mass [kg]
m_s	standard mass [kg]
z	vertical displacement [m]
$\ddot{z}$	vertical acceleration [m/s^2]
t	time [s]

III. HYDRODYNAMICS OF POINT ABSORBERS

The behavior of a point absorber can be studied similar that of a mechanical mass spring damper system. The system is considered to have one degree of freedom, i.e heave and to be acted upon by an external excitation force, i.e wave force. These concepts are extensively discussed in [12] and [13].

A. Equation of Motion

Let us consider a system having a coefficient of damping b_d and an external harmonic force with an amplitude F_A and angular frequency ω is applied on it. Then, the equation of motion for the system will take the form:

$$m\frac{d^2z}{dt^2} + b_d\frac{dz}{dt} + kz = F_A\sin(\omega t) \tag{1}$$

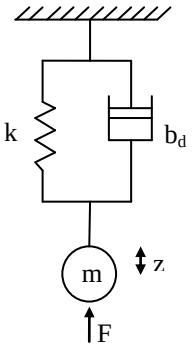

Fig. 2 A mass-spring-damper system

On solving, we get the critical damping coefficient,

$$b_c = 2\sqrt{km} = 2m\omega_n \tag{2}$$

Where, the natural frequency of the system is given by:

$$\omega_n = \sqrt{\frac{k}{m}} \tag{3}$$

The ratio of the damping coefficient to the critical damping coefficient is called the damping ratio, ζ_d

$$\zeta_d = \frac{b_d}{b_c} \tag{4}$$

The motion of the concerned point absorber is assumed to be heaving mode only. If the buoy makes a vertical displacement of z from mean position, the equation of motion of point absorber is:

$$m\frac{d^2z}{dt^2} = F_{ex} + F_{rad} + F_{res} + F_{hyddamp} + F_{exdamp} \tag{5}$$

Where, m is the combined mass of the buoy and the load above it and $\frac{d^2z}{dt^2}$ is its acceleration in heave direction. F_{ex} is the excitation force , F_{rad} is the radiation force, F_{res} is the restoring force given by the difference between buoyancy force and gravity force, $F_{hyddamp}$ is the hydrodynamic damping and F_{exdamp} is the external damping force imparted by the PTO mechanism.

For smaller diameter buoys, radiation effects are negligible therefore radiation force, F_{rad} is overlooked in the present work. However, during scaling up, one may have to consider the effects of radiation as well.

$$F_{res} = \rho V(t) - mg \tag{6}$$

Where ρ is the density of water and $V(t)$ is instantaneous draft volume.

Assuming damping forces to be linear,

$$F_{hyddamp} = b_{hyd} \frac{dz}{dt} \tag{7}$$

$$F_{exdamp} = b_{ex} \frac{dz}{dt} \tag{8}$$

Where, b_{hyd} and b_{ex} are called damping coefficients.

B. Response Amplitude Operator

The Response Amplitude Operator is the ratio of the heave amplitude of the buoy to the wave amplitude. RAO establishes a relationship between the input and output characteristics of a point absorber. RAOs play an important role in designing a WEC with maximum power absorption. For a point absorber, since heave motion is responsible for power generation, RAO can be calculated as:

$$RAO = \frac{\zeta}{\eta} \tag{9}$$

Where ζ is the amplitude of heave motion of the buoy and η is the amplitude of the wave.

C. Capture Width

Capture width is another performance parameter of a wave energy converter. It is the crest length of a wave which carries the same power as is absorbed by the wave energy converter.

$$\lambda = \frac{P_{abs}}{P_{wave}} \tag{10}$$

Where, P_{abs} is the absorbed power (W) and P_{wave} is the power of the incoming wave (W/m of the crest). However, the net power produced by system can also be used in place of absorbed power.

IV. Design Overview

This WEC system comprises of a buoy, a spar, a heave plate stand, and a PTO mechanism. The present work uses a similar MMR based power takeoff mechanism as proposed by *J. Ai et al* [11] but in a more efficient way that will result in higher efficiency and lower manufacturing, installation and maintenance costs. An MMR based PTO system converts the up and down motion of the buoy into a unidirectional rotational motion at the generator end. Unlike existing direct drive WECs, which uses a heavy, unreliable, costly and difficult to maintain linear generators; the proposed system uses a much more efficient rotary generator. Also, when compared to other indirect drive mechanisms, the proposed system proved to be more efficient.

Stainless steel SAE 316 was chosen as the fabricating material owing to its corrosion resistance, weldability, strength, workability, and availability. A scaling factor of 1:6.6 is chosen to fabricate a prototype for the proposed system. All the experiments and simulations are done for the scaled model. A CAD design of the prototype used for testing is shown in the left side of Fig. 3 and the PTO mechanism used is shown on the right side of Fig. 3.

A. Buoy

The buoy is manufactured in the shape of a cylinder with a diameter of 600mm, a height of 400mm and a thickness of 2mm. The buoy weighs around 30kg and can provide buoyancy more than 50kg. A linear bearing is fitted inside the buoy so that it can reciprocate on the spar with minimal friction. Two clamps are fitted on top of the buoy in order to fix the PTO mechanism. The stability test was often performed on the buoy during fabrication.

B. Spar

Spar is a cylindrical component passing through the buoy about which the buoy reciprocates. It supports the weight of generator and gears. In the full-scale design, the spar is to be made separately buoyant from the buoy. However, in the prototype, the spar is made from a Stainless Steel hollow tube with 48mm outer diameter, 42mm inner diameter, and 2m in length.

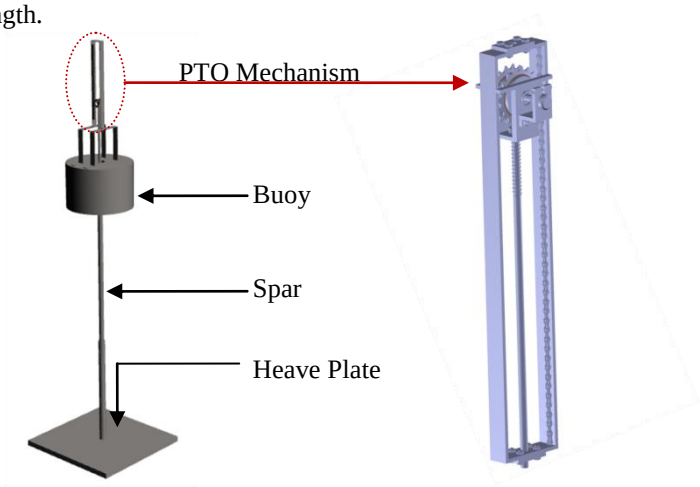

Fig. 3 The whole assembly and the PTO system

C. Heave Plate

Heave plate provides a counter force to the buoy motion and is responsible for a relative motion that is used for power conversion. This is achieved by means of weight and drag due to its large surface area. The spar is attached to the heave plate by means of a height adjusting mechanism. In the actual design, heave plate will be floating. However, due to the limitations in the depth of test facility, the heave plate of the prototype is fixed at the bottom. In the prototype, heave plate stand consists of a 1m square plate welded on the bottom of an SS tube with 50mm Inner diameter and 55mm outer diameter.

D. PTO Mechanism

The Power Takeoff Mechanism consists of two pairs of rack and pinion. The pinions are mounted on the shaft using one-way clutches that will transfer motion only in one direction of rotation. The pinions are mounted in such a way that when one pinion is engaged with its mating rack, the other will simply slide over its own. Thus, the output shaft will always rotate in the same direction. The output shaft of the prototype is coupled to a 25W DC generator, which in turn produces usable electricity. The pinions are connected to the spar using a ball joint so that small misalignments at the time of wave impinging can be taken care of.

V. Experimental Setup

A. Wave Flume

Experiments requiring wave generation are carried out in the 4m deep-water wave flume at IIT Madras. The length of the facility is 110m, width is 8m, and the water depth is 3.5m. The paddle of the wavemaker can be used as either piston type or flap type. Flap type paddle is used for the present work so that deep-water assumption can be made comfortably. The facility is capable of generating regular and random waves with wave height ranging from 5cm to 30cm and wave period ranging from 1s to 3s. However, only regular waves are considered in the present work. Wave absorber is installed at the other end to reduce the reflected wave effect. The prototype is installed in the flume as shown in Fig. 4

Fig. 4 Prototype installed in the flume

VI. Instrumentation

A. Displacement Measurement

Heave displacement of the buoy is measured by means of an accelerometer of sensitivity 1000 mV/g. The output of the accelerometer is read by using a Spider 8 Data Acquisition System.

B. Wave Height Measurement

Capacity type wave gauges are installed just before the buoy in order to capture the incident wave profile. Wave gauges are calibrated before each trial. Wave gauge signals are analyzed using the software programme catman.

C. Electric Power Output Measurement

In this wave energy converter, since the voltage and current changes instantaneously, microcontroller based digital measurement proved to be more effective. For the same reason, a DAQ system was assembled using Arduino UNO microcontroller and associated current and voltage sensors. The output can be seen on a computer screen simultaneously. A circuit diagram of the system is shown in Fig. 5.

D. Excitation force measurement

The excitation forces are measured while the buoy is held fixed with a varying period. The clamp is tightened very firmly so that the whole lifting force is transferred to the load cell. The load cell is connected to an Arduino microcontroller through an amplifier. Programming is done to calibrate the load cell and the value in N is displayed in the computer screen simultaneously. Fig. 6 shows the arrangement of load cell on top of the buoy.

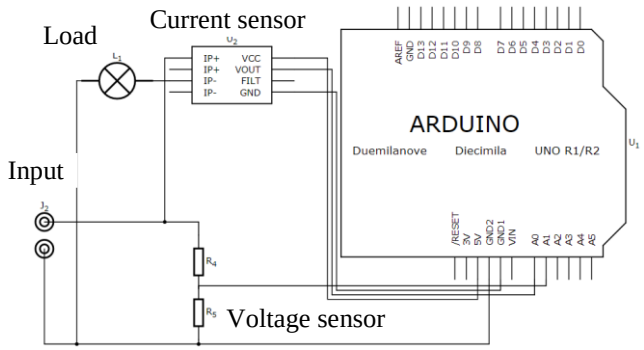

Fig. 5 Circuit diagram of the power measurement system

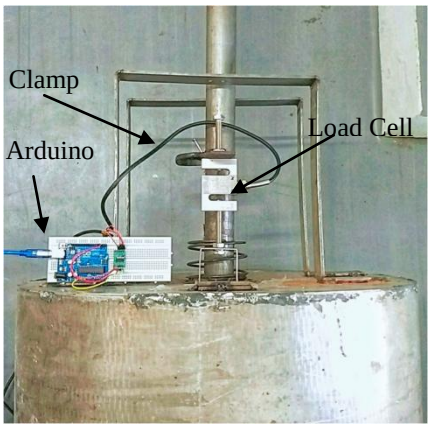

Fig. 6 Load cell arrangement

E. Friction Measurement

Since the present prototype uses rack and pinion as the PTO system, it is important to know the internal friction. The

frictional force is measured by using a setup as shown in Fig. 7. The pinion generator assembly is made to accelerate under the influence of known standard weights. Now, by energy balance, friction force can be calculated as:

$$F_{fric} = m_t \ddot{z} - m_s g \quad (11)$$

Where, m_t is the accelerated mass, m_s is the standard weight used and $\ddot{z}$ is the acceleration measured using an accelerometer.

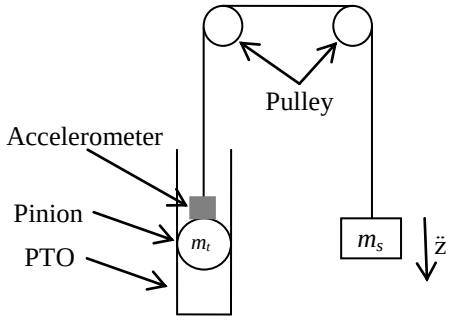

Fig. 7 Friction test setup

VII. Results And Discussions

A. Friction Test

Friction test revealed that the frictional force in the system is roughly 1.96N. By proper lubrication, these numbers can be improved.

B. Electrical Power Output Measurement

For a wider range, the power output was higher for higher wave height and lower wave period as expected. A typical power matrix obtained for different wave heights and periods is shown in Table 1.

TABLE I
Power Output (W) for Different Wave Heights And Periods

		Tp (s)		
		2	2.5	3
H (cm)	10	0.931	0.7875	1.1357
	12	3.685	2.31	2.214
	15	12.765	9.27	5.95
	17	18.088	10.028	10.752
	19	22.648	13.268	10.752

Fig. 8 shows the voltage output for a wave height of 15cm and a period of 1s. A peak voltage of 11V was generated. Each peak signifies either a crest or a trough encountered by the buoy.

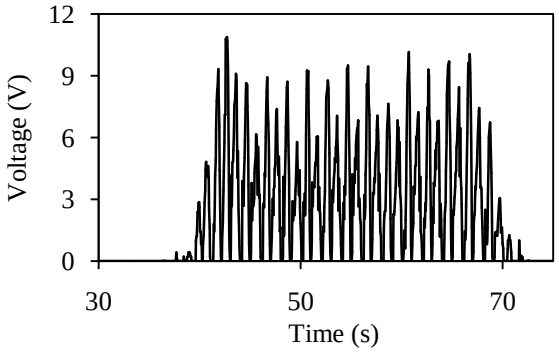

Fig. 8 Voltage output for a wave height of 15cm and a period of 1s.

C. Heave Displacement

Heave displacement is measured by using an accelerometer by double integrating its output. The response of the buoy for a wave height of 15cm and a period of 3s is shown in Fig. 9. A phase lag of approximately 60° is observed between the heave motion of the buoy and the wave. A heave displacement of 16.89cm is recorded at this particular wave conditions . Comparatively lower heave displacement can be due to a phase lag much lesser than 90° that is required for resonance. The heave displacement can go as high as 28cm at higher frequencies for the same wave height.

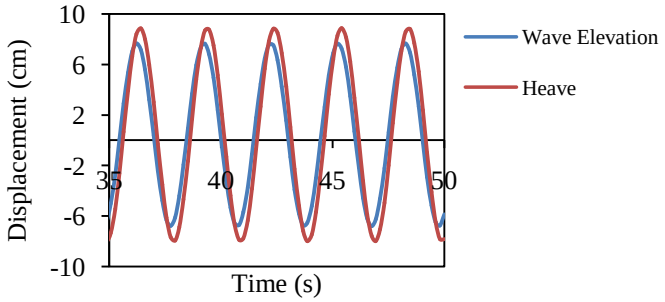

Fig. 9 Wave profile and the buoy position

D. Response Amplitude Operator (RAO)

RAO can be measured for all the three motions; heave, pitch and roll. However, in the case of a point absorber, heave motion is more significant. Hence, RAO for pitch motion is evaluated here. Fig. 10 shows the variation of RAO at different wave periods for a wave height of 15cm. It can be seen that the RAO has a maximum value at a particular frequency. This is because that particular frequency matches closely with the resonant frequency of the system.

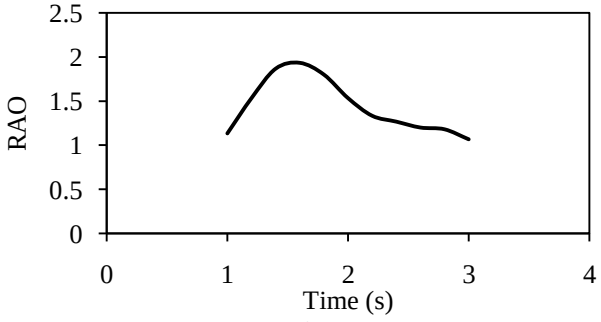

Fig. 10 RAO for heave motion

E. Capture Width

Fig. 11 shows the variation of capture width with different wave periods for a wave height of 15cm. It is seen that, beyond the critical frequency, the capture width decreases with an increase in the wave period. This is due to a reduction in power absorbed at lower frequencies. Dividing the capture width by the diameter gives the absorption efficiency.

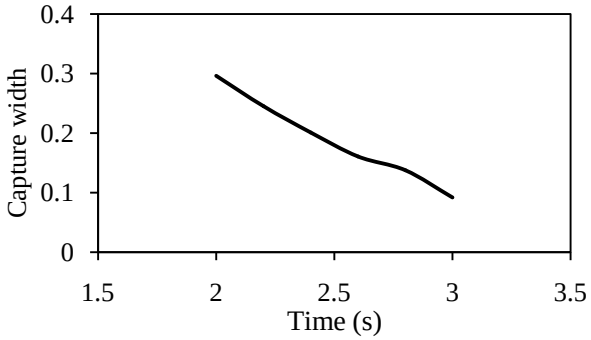

Fig. 11 Capture Width vs Time

Fig. 12 shows the variation of absorption efficiency with different wave periods for a wave height of 15cm. It shows the same trend as that of the capture width. A maximum efficiency of 50% is obtained for a period of 2s.

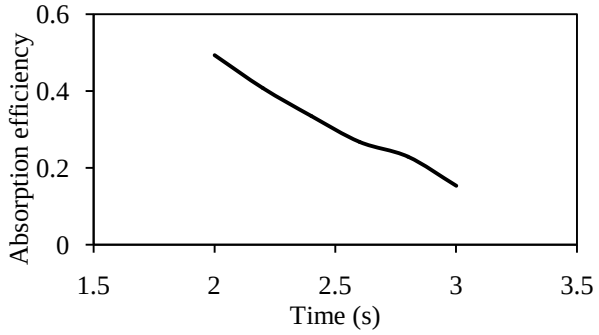

Fig. 11 Absorption Efficiency vs Time

VIII. CONCLUSIONS

It is evident from the experiments that the power extracted by the WEC is maximum for a wave with a wave period of 2s and wave height of 19cm. Even though the range of wave period and wave height tested is limited by the capacity of the wave maker, it can be generally stated, as the power absorption is maximum at higher wave height and higher wave frequency. Using Froude scaling law, scaling up the diameter of the existing buoy to 5 meters gave an average power of about 16 kW and a peak power of 33 kW.

The system is found to have a maximum absorption efficiency of 50% for a wave period of 2s. Efficiency can be increased further by improving the design.

Phase control techniques can be used to improve the power absorption at a wide range of frequencies.

ACKNOWLEDGMENT

This work was supported under the Innovative Projects by IIT Madras [ICS/16-17/831/RR1E/MAHS].

REFERENCES

[1] J. Cruz, *Ocean Wave Energy Current Status and Future Prepectives*. 2008.

[2] A. F. d. O. Falcão, "Wave energy utilization: A review of the technologies," *Renew. Sustain. Energy Rev.*, vol. 14, no. 3, pp. 899–918, 2010.

[3] A. Clément *et al.*, "Wave energy in Europe: Current status and perspectives," *Renew. Sustain. Energy Rev.*, vol. 6, no. 5, pp. 405–431, 2002.

[4] K. Budar and J. Falnes, "A resonant point absorber of ocean-wave power," *Nature*, vol. 256, no. 5517, pp. 478–479, 1975.

[5] "Handbook of Ocean Wave Energy," vol. 7, 2017.

[6] T. K. Das, P. Halder, and A. Samad, "Optimal design of air turbines for oscillating water column wave energy systems : A review," *Journal of Ocean and Climate*, vol. 8, no. 1, pp. 37-49, 2017.

[7] R. Henderson, "Design, simulation, and testing of a novel hydraulic power take-off system for the Pelamis wave energy converter," *Renew. Energy*, vol. 31, no. 2, pp. 271–283, 2006.

[8] M. Leijon *et al.*, "Wave energy from the north sea: Experiences from the lysekil research site," *Surv. Geophys.*, vol. 29, no. 3, pp. 221–240, 2008.

[9] H. B. Karayaka, H. Mahlke, D. Bogucki, M. Mehrubeoglu, A. Texas, and M. U. Christi, "A Rotational Wave Energy Conversion System Development and Validation with Real Ocean Wave Data," no. 140130, pp. 5–11, 2011.

[10] J. Sjolte, G. Tjensvoll, and M. Molinas, "Power Collection from Wave Energy Farms," pp. 420–436, 2013.

[11] J. Ai, L. Zuo, H. Lee, and C. Liang, "Design, Fabrication, Simulation and Testing of a Novel Ocean Wave Energy Converter," *ASME Int. Manuf. Sci. Eng. Conf.*, vol. 1, pp. 1–7, 2015.

[12] S.K. Chakrabarti, "Hydrodynamics of Offshore Structures", *Computational Mechanics Publications*, 1987.

[13] J. Falnes, *Ocean Waves and Oscillating Systems: Linear Interaction Including Wave Energy Extraction, Cambridge, UK*. 2002.